

A COMPARISON OF KINETIC IMPACTOR AND NUCLEAR DEFLECTION FOR A BENNU-LIKE OBJECT.John Michael Owen¹, M.Bruck Syal¹, C.D. Raskin¹, D.S. Dearborn¹, N. Melamed²,¹Lawrence Livermore National Laboratory, mikeowen@llnl.gov;²The Aerospace Corporation**Keywords:** *asteroid, hazard mitigation, simulations, failure and fracture modeling*

This study presents a detailed modeling comparison of asteroid diversion using kinetic impactors and stand-off nuclear energy deposition in 3D. We apply our compatibly differenced (exactly energy conserving) ASPH (Adaptive Smoothed Particle Hydrodynamics) modeling code *Spherical* to study this problem [Owen et al., 1998; Owen, 2010, 2014]. We use a “Bennu-like” object as our NEO target. This object is based on the radar shape information for Bennu (approximately 494 meters in diameter), but assumes a simple monolithic porous internal structure with a Tillotson granite equation of state. We assume an initial uniform porosity of $\phi = 25\%$, yielding an initial bulk density of $\rho_o = 2.01 \text{ g/cm}^3$. In reality Bennu has a carbonaceous chondritic composition with a higher porosity than we assume here, but our motivation is to examine a representative object rather than Bennu specifically.

We begin by considering a 10 ton kinetic impactor striking the asteroid at 15 km/sec. Fig. 1 shows the state of the damage and velocity of the ejecta leaving the surface 0.25 seconds after impact. *Spherical* uses

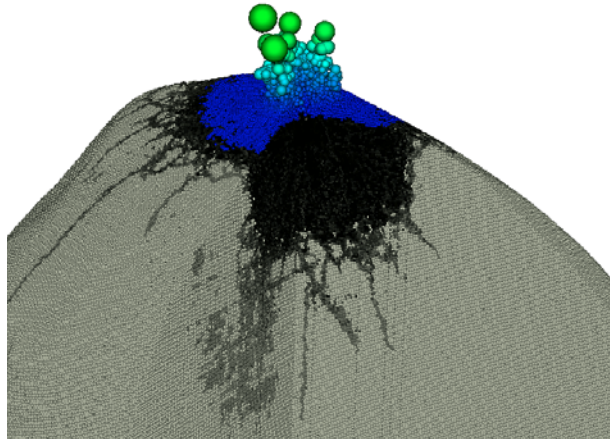


Figure 1: Trace of the damage tensor (grey scale) and velocity of ejecta (colored) 0.25 seconds after the impact of 10 ton kinetic impactor at 15 km/sec. One quadrant of the asteroid has been removed to allow visualization of the interior damage.

a tensor damage model, so the gray scale varies from darkest where the material is completely rubblized immediately under the crater, to lighter values where the

damage is dominantly in a single direction in fractures radiating away from the impact point. We show in Fig. 2

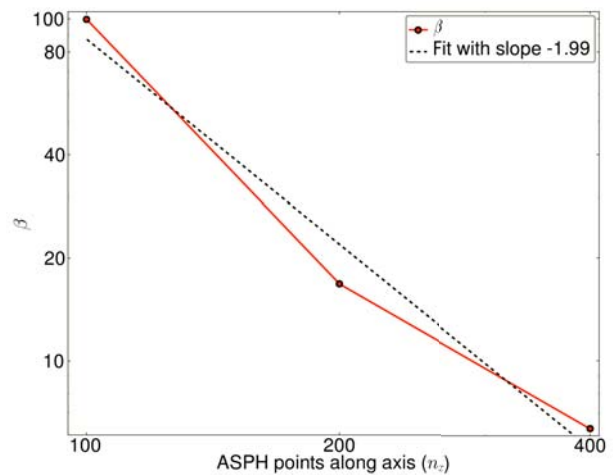


Figure 2: Convergence of the momentum magnification factor β as a function of linear resolution for the kinetic impactor scenario.

the strong dependence of the momentum magnification factor $\beta \equiv 1 + p_{\text{ejecta}}/p_{\text{impactor}}$ on the spatial resolution. Note that our highest resolution calculation ($n_x = 400$ points across the equator for a spatial resolution of $h \sim 2\text{m}$) requires 20×10^6 ASPH points. We find that β converges at second-order using our method. This is confirmed in a previous study by Owen [2014], where we also find the standard SPH energy evolution form only converges at first-order for this kind of deflection metric. Applying Richardson extrapolation to estimate our final converged value we find $\beta = 2.8 \pm 0.7$ and a total deflection velocity of $v_d = 0.31 \pm 0.08 \text{ cm/sec}$.

We find the dominant sensitivity in determining β for our kinetic impactor models is the mass of the material ejected (see Fig. 3) – under-resolved calculations find much larger ejecta masses. This is consistent with our previous experience [Rovny et al., 2013] that under-resolved models tend to damage the material too extensively, allowing more mass to be eligible for ejection.

We next consider the deflection of this same object using X-ray deposition from a standoff nuclear explosion. In this case we assume a 1 Mt source sitting 350 m from the center of the asteroid off the equator: this yields a

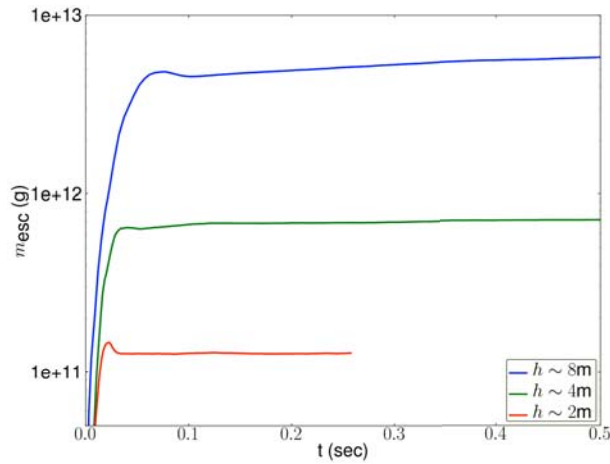


Figure 3: Time histories of the total mass ejected from the asteroid for three resolutions of the kinetic impactor calculation.

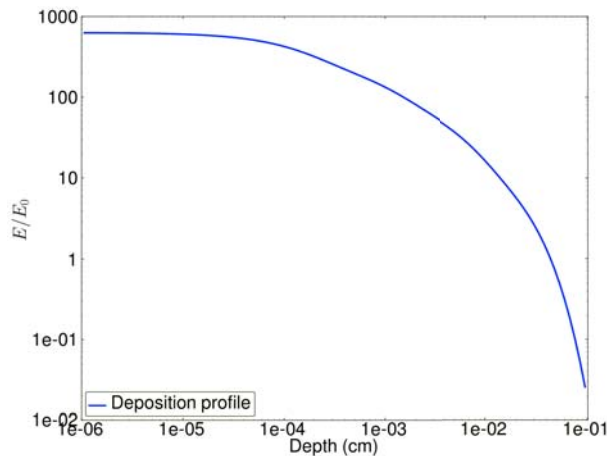


Figure 4: Fitted deposition profile as a function of depth due from a 2 keV X-ray source. See Managan et al. [2015].

distance of 88 m from the closest point on the surface. Fig. 4 shows the energy deposited as a function of depth from a monochromatic 2 keV source of X-rays found by Managan et al. [2015]. This profile requires resolutions at the surface of 10’s of μm , imposing difficult resolution requirements for a 3D model such as we wish to use here. We accomplish this by using ASPH’s flexibility to allow different resolutions in different directions. We model a 10m deep “skin” of the asteroid for any facets of the shape model that see the source. For each of these facets we extrude ASPH points inward 10m, ratioing the spacing of the points in depth from the surface such that a desired surface depth resolution is achieved. We consider models with surface resolutions $h_{\text{surface}} \in [10\mu\text{m}$,

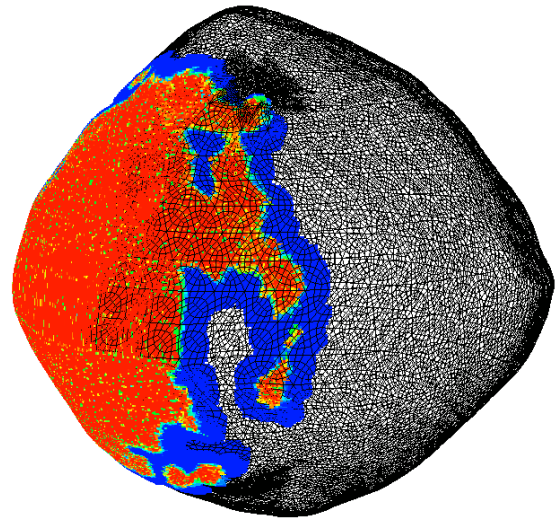


Figure 5: Logarithm of the specific energy after the initial deposition of the energy for the nuclear stand-off simulations. For clarity we have added a small sphere at the position of the source (on the left) and the polyhedral surface shape of Benu: the ASPH simulations are only of the colored skin regions depicted.

$100\mu\text{m}$, 1mm, & 1cm], i.e., changing by a factor of 10 at each step. We maintain a resolution across the surface of 2m in all cases, implying for our finest resolved cases we are allowing aspect ratios of order 10,000 in the ASPH resolution shapes at the surface. Fig. 5 shows the logarithm of the surface energies at the start of one of these calculations. You can clearly see the effect of the irregular polyhedral surface in which facets are exposed to the source, which also influences the amount of energy deposited in the material under each facet.

Fig. 6 shows the time histories of the deflection velocity for our models of the nuclear stand-off scenario. We again find sensitivity in the deflection velocity to resolution, though in this case the mechanisms are subtly different than those of the kinetic impactor. The convergence of these curves is complicated by the fact that each calculation actually uses the same number of points: we achieve finer surface resolutions by increasing the ratioed spacing of points, trading off finer surface resolution for coarser interior representations. The factor controlling how much material is blown-off is how deeply the energy source penetrates: specifically how deeply the material is heated above melt so that it can blow-off. We find with coarsening resolution that we overestimate how much material is coming off and therefore overestimate the deflection. Effectively with overly coarse resolutions we are overestimating

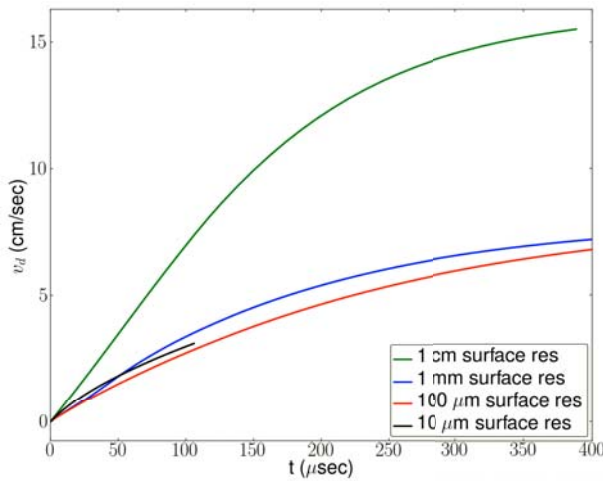


Figure 6: Time histories of the deflection velocity for models of the nuclear deposition scenario.

how deeply the energy penetrates. For instance in the $h_{\text{surface}} = 1 \text{ cm}$ case all the energy is deposited in the first shell of points equating to a penetration depth of 0.5 cm, far more than the profile of Fig. 4 indicates should occur. Eventually coarse enough calculations will reverse this trend: at the point where the surface resolution is large enough that the input energy cannot melt the first numerical layer of material. The finer resolution calculations are converging to roughly 6 cm/sec deflection for this initial blow-off of super-heated material.

It is also worth noting that the blow-off creating the initial deflection velocity is not the end of the story for the nuclear scenario. There is a strong shock that has only propagated inward roughly 2m by the 400 μsec at which we terminate our simulations. Much like the kinetic impactor case we expect this shock will damage and eject more material as it moves inward, enhancing the deflection velocity. We are in the process of mapping these initial high-resolution “skin” calculations to models of the whole object in order to follow the shock and damage dominated next stage. The results of this study should have interesting implications for understanding the distinction between deflecting an object and disrupting it, as for small enough objects/energetic enough sources disruption could be a distinct possibility.

We can use these scenario based deflection velocities (0.31 cm/sec for the kinetic impactor and 6 cm/sec for nuclear) to estimate the outcome of deflection efforts for the PDC scenario orbit. Table 1 shows the outcome for several possible interception times. For an object as large as our Bennu-like case our 10 ton, 15 km/sec kinetic impactor is unable to deflect the object. The 1 Mt source is only able to successfully deflect the object for

Years to impact	Kinetic Impactor	Nuclear
4.70	0.22	4.2
2.51	0.12	2.2
1.43	0.066	1.3
0.39	0.027	0.52

Table 1: Deflection predictions (in Earth radii) for the PDC scenario orbit for various intercept times for our model Bennu-like object.

interception times of at least a year out assuming our 88m height of burst. We expect of course for smaller objects/longer lead times the kinetic impactor is a viable option. Similarly larger nuclear sources or different standoff distances could provide more options even for late time interceptions.

Acknowledgments

Part of this work was funded by the Laboratory Directed Research and Development Program at LLNL under project tracking code 12-ERD-005, performed under the auspices of the U.S. Department of Energy by Lawrence Livermore National Laboratory under Contract DE-AC52-07NA27344. LLNL-ABS-669389.

References

R A Managan, K M Howley, and J V Wasem. Efficient and Accurate Mapping of Nuclear-Energy Deposition. In *4th IAA Planetary Defense Conference – PDC 2015*, Frascati, Italy, 2015.

J Michael Owen. ASPH modeling of Material Damage and Failure. In *Proceedings of the 5th International SPHERIC Workshop*, Manchester, UK, 2010.

J Michael Owen. A compatibly differenced total energy conserving form of SPH. *International Journal for numerical methods in fluids*, 75(11):749–774, April 2014.

J Michael Owen, Jens V Villumsen, Paul R Shapiro, and Hugo Martel. Adaptive Smoothed Particle Hydrodynamics: Methodology. II. *The Astrophysical Journal Supplement Series*, 116(2):155–209, June 1998.

J Rovny, J M Owen, K Howley, and J Wasem. Modeling Impact Cratering on Phobos. In *44th Lunar and Planetary Science Conference*, The Woodlands, TX, 2013.